Short title: S1 Reorganization BDNF & TrkB

Reorganization of the Somatosensory Cortex: Brain-Derived Neurotrophic Factor (BDNF) and High Affinity Receptor TrkB

Sarah L. Chollar

Systems Neuroscience Program

Psychology Department

Master's Thesis

Abstract

Neural plasticity allows the brain to adapt to changes brought on by experience, trauma, and disease. Previous research has described many anatomical and physiological alterations that are associated with neural plasticity and cortical reorganization including the remodeling of synapses, dendritic arbors, and growth of axons, as well as changes in synaptic efficacy including long and short-term potentiation and depression. Brain-derived neurotrophic factor (BDNF) has emerged as a promising candidate molecule that may provide a link between the anatomical and physiological changes observed during reorganization of the cortex. In this study, we have used *in vivo* electrophysiological techniques to map the border between the forepaw and lower jaw representations in the rat somatosensory cortex, and immunohistochemical techniques to identify the distribution of BDNF and high-affinity receptor TrkB at the border and within the forepaw and lower jaw representations during reorganization induced by peripheral denervation. Initial results reveal statistically significant layer specific differences in antibody staining for BDNF at the border compared to the forepaw and lower jaw representations in normal acute controls.

Reorganization of the Somatosensory Cortex: Brain-Derived Neurotrophic Factor (BDNF) and High Affinity Receptor TrkB

The mammalian brain is a highly organized structure; specific sensory systems are associated with defined cortical areas including primary visual (V1), auditory (A1), and somatosensory cortices (S1; Calford, 2002; Kaas, 2008). In these primary sensory cortices, information is organized topographically creating distinct 'maps' of the retina, cochlea, and surface of the body (Calford, 2002; Rosa and Tweedale, 2005; Schreiner and Winer, 2007). Tactile sensory information from the periphery is processed in S1, and is organized such that adjacent parts of the body are represented in adjacent cortical areas of S1. In this way, S1 forms a map representing the entire body surface. The cortical representations of the body are maintained by peripheral input, and therefore are highly dynamic and capable of change in response to changes in activity (Calford, 2002). Neural plasticity may broadly be defined as the ability of the central nervous system to undergo changes and adapt in response to environmental stimuli, experience, disease and injury (Flor et al., 2006; Irvine, 2007: Ludlow et al., 2008).

Neural plasticity and cortical reorganization following amputation have been well documented (Lotze et al., 2001; Woodhouse, 2005; Flor et al., 2006). Following the amputation of a limb, reorganization takes place in S1 as adjacent representations expand into areas of the deafferented cortex (Lotze et al., 2001). Several neural imaging studies have found a positive correlation between phantom limb pain and cortical reorganization (Moore et al., 2000; Lotze et al., 2001; MacIver et al., 2008); as the extent of cortical reorganization increases, so does the probability of phantom pain. The treatment of phantom limb pain has traditionally been a challenging clinical issue (Woodhouse, 2005; Flor et al., 2006); in understanding the mechanisms that underlie phantom limb phenomena we will be able to design new treatments to

prevent and ameliorate the often debilitating and persistent pain experienced by people who have been amputated (Woodhouse, 2005; Flor et al., 2006; Acerra et al., 2007; MacIver et al., 2008).

Plasticity has been well studied in visual, auditory, and somatosensory systems (Prakash et al., 1996; Calia et al., 1998; Cheetham et al., 2007, 2008; Irvine, 2007; Oh et al., 2007; Tan et al., 2007). Experimental manipulations involving enhanced sensory experience and sensory deprivation throughout development have highlighted the important contributions of sensory experience, especially during critical periods (Van der Loos and Woolsey, 1973; Singh et al., 1997; Calia et al., 1998; Berardi et al., 2000; Daw et al., 2007). Much research has focused on the whisker barrel representation in the rodent somatosensory system (Woolsey et al., 1975; Steffen and Van der Loos, 1980; Prakash et al., 1996; Calia et al., 1998; Daw et al., 2007; Cheetham et al., 2007, 2008). Deprivation of sensory experience induced by whisker trimming or plucking results in different forms of plasticity and reorganization in the somatosensory cortex over the course of development (Steffen and Van der Loos, 1980; Singh et al., 1997). Early deprivation of whisker experience alters the morphology of layer IV whisker barrels in the rat and mouse (Van der Loos and Woolsey, 1973; Steffen and Van der Loos, 1980; Singh et al., 1997; Calia et al., 1998; Daw et al., 2007). After the critical period has ended, deprivation in the juvenile and adult is capable of inducing functional physiological changes; however, it does not alter the gross morphology of whisker barrels (Singh et al., 1997; Cheetham et al., 2007; Daw et al., 2007). Stimulating the whiskers also produces functional as well as structural changes in layer IV whisker barrel representations; direct stimulation of individual whiskers or loss of surrounding whiskers leads to the expansion of spared barrel representations at the expense of surrounding or deprived barrels (Steffen and Van der Loos, 1980). Application of exogenous neurotrophins, or growth factors, to the deprived whisker pad can maintain the deprived barrel

representations in neonatal rats (Prakash et al., 1996; Calia et al., 1998). Environmental enrichment has also been shown to affect the morphology of neurons found in whisker barrel representations in the somatosensory cortex; including changes in the size, shape, and density of dendritic spines, as well as changes in synapse size and number (Markham and Greenough, 2004). Together these studies provide examples of activity-dependent plasticity and cortical reorganization throughout development, as well as illustrate the importance of sensory experience and peripheral input in generating and maintaining the somatotopic organization in S1.

Plasticity and cortical reorganization are associated with many changes in both the structure and function of S1. Remodeling of dendritic arbors and growth of axons have been observed following peripheral denervation and sensory deprivation (Steffen and Van der Loos, 1980; Jain et al., 1998; Hickmott and Merzenich, 1998; Calford, 2002; Hickmott and Steen, 2005; Hickmott and Ethell, 2006; Cheetham et al., 2008); these changes are associated with reorganization and translocation of the border between the deafferented and adjacent representations. Functional changes are also observed following peripheral denervation, as adjacent representations expand into deprived cortical areas (Cheetham et al., 2007). Changes have been observed in local circuit properties (excitation and inhibition) as well as the intrinsic properties of neurons during reorganization of the forepaw and lower jaw representations in S1 (Hickmott and Merzenich, 1998, 2002; Hickmott, 2005). Axons and dendrites typically display an orientation bias near representational borders (Steffen and Van der Loos, 1980; Calford, 2002; Hickmott and Steen, 2005; Steen et al., 2007); excitatory and inhibitory postsynaptic currents are weaker when evoked from across these representational borders indicating a physiological bias in addition to the anatomical bias (Petersen and Sakmann, 2000).

Neurotrophins, a family of secreted diffusible growth factors, include brain-derived neurotrophic factor (BDNF), nerve growth factor (NGF), neurotrophic factor 3 (NT-3), and neurotrophic factor 4/5 (NT-4, NT-4/5; for reviews, see Bibel and Barde, 2000; Huang and Reichardt, 2001; Sofroniew et al., 2001; Lu, 2003). Each of the neurotrophins bind to a cognate receptor in the tropomyosin related kinase (Trk) family of receptor tyrosine kinases (Bibel and Barde, 2000; Huang and Reichardt, 2001; Sofroniew et al., 2001). NGF binds to TrkA, BDNF and NT-4/5 bind with equal affinity to TrkB; while NT-3 binds with high affinity to TrkC, it also activates TrkB receptors (Lindsay et al., 1994). Each of the neurotrophins (BDNF, NGF, NT-3, and NT-4/5) bind with equal affinity to the $P75^{NTR}$ receptor (for reviews, see Dechant and Barde, 1997; Hempstead, 2002). The $P75^{NTR}$ receptor has a role in triggering apoptosis, as well as enhancing the specificity of neurotrophin signaling (Dechant and Barde, 1997; Hempstead, 2002). Binding of BDNF to its cognate receptor TrkB triggers autophosphorylation of the intracellular tyrosine residues. Autophosphorylation of specific intracellular tyrosine residues may activate one or more of the major intracellular signaling pathways (Nagappan and Lu, 2005).

BDNF has emerged as a promising candidate molecule that may provide a link between the anatomical and physiological changes observed during cortical reorganization. Several converging lines of evidence indicate that BDNF meets the criteria necessary for such a molecule. Transcription and release of BDNF is activity-dependent (Shieh and Ghosh, 1999), capable of modulating synaptic transmission (Lu, 2003; Zhang et al., 2008) and can influence the growth of axons and remodeling of dendritic arbors (McAllister, 2000, 2001).

Many studies support the activity-dependent release of BDNF (Prakash et al., 1996; Lu, 2003). Release of BDNF may take place as classic anterograde release from synaptic buttons, as

well as retrograde release from postsynaptic dendrites, acting as both an autocrine and paracrine signal (Cabelli et al., 1996; Yan et al., 1997b; Pitts and Miller, 2000; Lipsky and Marini, 2007). BDNF is capable of modulating inhibition and enhancing glutamatergic synaptic transmission (Prakash et al., 1996; Lu, 2003). During development, BDNF plays many important roles in the growth of the nervous system including roles as a survival factor to a key regulator in synapse formation (Huang and Reichardt, 2001; Lipsky and Marini, 2007). In periods of development the limited quantities of neurotrophins act as survival factors, enhancing the growth of axons and dendrites (McAllister, 2000, 2001). Many studies have highlighted the important roles of BDNF and TrkB during development of the somatosensory cortex (Singh et al., 1997; Calia et al., 1998; Lush and Parada, 2005). Using BDNF, NT-4, and TrkB transgenic mutant mice, researchers have shown that during the development of the barrel cortex, TrkB signaling is required for normal patterning of thalamic input to layer IV (Lush and Parada, 2005). Throughout the lifetime, BDNF plays important roles in the maintenance of neurons by promoting cell growth and survival, as well as influencing neural transmission and synaptic plasticity (Prakash et al., 1996; Yan et al., 1997b; Huang and Reichardt, 2001; Lipsky and Marini, 2007).

Several studies have utilized immunohistochemical techniques to identify the distribution of neurotrophins in the cortex (Yan et al., 1997a, 1997b; Miller and Pitts, 2000; Pitts and Miller, 2000). These studies have shown that several neurotrophins including NGF, BDNF, and NT-3 are widely distributed throughout the cortex, and are found in approximately equal proportions (Pitts and Miller, 2000). In addition to the wide distribution of multiple neurotrophins in the cortex, individual neurons have been shown to express multiple neurotrophins and Trk receptors (Miller and Pitts, 2000; Pitts and Miller, 2000). Layer specific patterns of neurotrophin expression have also been observed. For NGF, BDNF, and NT-3, the greatest amount of staining

is consistently observed layers II/III, V, and VI (30 % of neurons labeled), while the lowest proportion of antibody staining appears in layer IV (5-10 % of neurons labeled, Yan et al., 1997b; Miller and Pitts, 2000; Pitts and Miller, 2000). Pitts and Miller (2000) also examined the coexpression of neurotrophins with their high-affinity Trk receptors and found nearly 70 % of neurons positive for a neurotrophin were also expressing the cognate high-affinity Trk receptor.

Studies in the visual system have also highlighted important roles for BDNF and TrkB during plasticity, including the involvement of TrkB in recovery of cortical responses following monocular deprivation, and BDNF and TrkB signaling involvement in LTP of inhibitory synapses of visual cortical pyramidal neurons (Inagaki et al., 2008; Kaneko et al., 2008). Application of exogenous NGF does not influence the normal development of ocular dominance columns, or influence plasticity following monocular deprivation (Silver et al., 2001); however infusions of NT-4/5 during the critical period can rescue responses following monocular deprivation (Gillespie et al., 2000). Studies have also examined the roles of BDNF and TrkB during the development of the visual system, where the expression of TrkB is located on axons early in development, and shifts to cell bodies and dendrites in later stages of development as cells mature (Cabelli et al., 1996).

In the auditory system, several studies have examined the role of neurotrophins during auditory plasticity. Tan et al. (2007), induced auditory trauma by presenting pure-tones, and found that BDNF protein levels and mRNA expression were upregulated in the inferior colliculus, while simultaneously downregulated in the auditory cortex. Further studies of the *bdnf* gene found initial downregulation following cochlear ablation at 2 weeks, followed by an increase in *bdnf* gene expression at 4 weeks, and downregulation again at 12 weeks (Oh et al., 2007). Taken together, these studies of the somatosensory, visual, and auditory systems support

the role of BDNF as a promising candidate molecule that may link anatomical and physiological changes observed during cortical plasticity and reorganization.

In order to study the role of BDNF during reorganization of the adult somatosensory cortex, we are using a model system that allows for *in vivo* mapping of the somatosensory cortex in the anesthetized rat to determine the location of the border between the forepaw and lower jaw representations. Groups will consist of experimental (denervated), sham denervation, and acute controls. In experimental groups, cortical reorganization is induced by peripheral denervation; in sham controls the nerves are examined but remain intact. A second mapping procedure is then conducted on experimental and sham groups at three, seven, or fourteen day time points to determine the extent of cortical reorganization at the border of the forepaw and lower jaw representations. Immunohistochemistry is then used to determine the distribution of BDNF and TrkB fluorescent antibody labeling in serial tissue sections taken from the border region of the somatosensory cortex. Images are acquired for further processing and statistical analysis. Using these methods, we will be able to characterize the distribution of BDNF and TrkB antibody labeling in S1 in normal and reorganized groups, as well as identify changes taking place over time.

We are specifically seeking to (1.) determine the distribution and compare antibody staining for BDNF and TrkB at the border and within the forepaw and lower jaw representations in normal acute control, experimental, and sham groups, (2.) examine potential changes in antibody labeling over time using 3-day, 7-day, and 14-day time points for experimental and sham groups, and (3.) assess the potential effects of the dye mark on antibody staining distribution.

Materials and Methods

Animals

Female adult Sprague-Dawley rats (P 160-210) were bred and maintained under standard housing conditions (group housing preoperatively, individual housing postoperatively); 12 hour day/night cycle, food and water available *ad libidum*.

Surgical Preparation

All procedures were approved by the University of California, Riverside Institutional Animal Care and Use Committee (IACUC). Aseptic conditions were maintained for all recovery surgical procedures. Animals were anesthetized by intraperitoneal (IP) injection of dilute pentobarbital (0.25 mL/100 g) until areflexic, supplementary anesthesia was administered throughout the procedure when necessary as assessed by hindpaw withdrawal response. Once anesthetized, animals were placed on a homeothermic blanket (Homeothermic Blanket Control Unit, Harvard Apparatus) to maintain temperature (35-37° C), and positioned in a stereotaxic device (David Kopf Instruments). Experimental and sham groups received an additional IP injection of lactated ringers (approximately 2.5 mL; Abbot Laboratories) containing dexamethasone sodium phosphate (0.1 mL/1 kg, American Reagent Inc.), and a subcutenous (SC) injection of baytril (0.22 mL/1 kg, Bayer Health Care, LLC). Atropine sulfate (0.1 mL, AMTech Group, Inc.) was administered via IP injection every three hours throughout the procedure to all groups to reduce respiratory secretions. Prior to the initial incisions, 2% lidocane hydrochloride (Abbot Laboratories) was administered via SC injections to the scalp and left forearm.

In acute groups, a cisternal drain was opened, the temporal muscle retracted, and a rectangular craniotomy opened over the intersection of bregma and the temporal crest. The dura

mater was removed and the brain covered in silicone oil. In experimental and sham groups, the dura was left intact and covered with saline. A photograph was taken of the cortical surface using Pixera software (Pixera Corporation), and the locations of electrode penetrations were recorded on this image using Canvas 5 software (Deneba Software; Fig. 1).

Electrophysiology

Carbon fiber glass microelectrodes (7-10 μm diameter) were lowered into the cortex using a micropositioner (650D, Kopf Instruments) to layers III-IV ($\sim$580 μm recording depth) to record responses to cutaneous stimulation of the lower jaw and forepaw elicited by tactile stimulation with a glass probe. Multiunit responses were amplified using a microelectrode AC amplifier (Model 1800, AM-Systems), connected to an audio monitor (AM9, Astro-Med, Inc.), and the signal was band-pass filtered (300 Hz - 1 kHz). Responses were subjectively categorized as a lower jaw, forepaw, border (both forepaw and lower jaw), or no evoked response. Border sites located 200 μm apart in the rostral-caudal dimension were identified, and sites 500 μm from the border either medial or lateral were mapped (Fig. 1). Once several border and corresponding medial/lateral sites were identified, they were then marked with a fluorescent dye, 1,1′-dioctadecyl-3,3,3′,3′-tetramethylindocarbocyanine perchlorate (DiI, 1-2 % in ethanol, Molecular Probes; DiCarlo et al., 1996). Electrodes used for recording were dipped in the DiI solution until coated with crystals, and used to relocate and confirm the mapped border and corresponding medial/lateral sites; once confirmed, electrodes were left in place at the recording depth ($\sim$580 μm) for 2 min. Following the initial mapping in recovery animals, the craniotomy was covered with Gelfoam® (Pharmacia & Upjohn Company) and scalp sutured (DEXON™II absorbable sutures, COVIDIAN). During the second mapping procedure in experimental and sham groups, the border was relocated and 3,3′-dioctadecyloxacarbocyanine perchlorate (DiO, 1% in ethanol;

Molecular Probes) was used to mark the site of the reorganized border. Electrodes used for recording were repeatedly dipped until coated with DiO crystals, reintroduced to the cortex at the site of the reorganized border and left in place at the recording depth (∼580 μm) for 2 min.

Inducing Reorganization

Following the initial mapping procedure, experimental and sham groups were removed from the stereotaxic device (Kopf Instruments) and a denervation or sham-denervation procedure was performed. Lidocaine hydrochloride (2%) was SC injected into the forearm prior to incision, in sham groups the median and radial nerves were identified and examined, but left intact. In experimental groups, the median and radial nerves were identified, ligated to prevent regrowth, and severed to induce reorganization of the border between the forepaw and lower jaw representations (Hickmott and Merzenich, 2002; Hickmott, 2005; Hickmott amd Steen, 2005). Experimental and sham groups were then sutured, monitored until recovery from anesthesia, and returned to standard housing conditions (housed individually). Elizabethan collars were sometimes used in denervated groups to prevent or delay the onset of autotomy of the forelimb and digits.

In acute groups, following the *in vivo* electrophysiological mapping of the border of the forepaw and lower jaw, animals were given a lethal dose of pentobarbital (0.2 mL in 0.8 mL saline) and transcardially perfused with 10 % buffered formalin phosphate. Hemisected brains were postfixed overnight in 10 % buffered formalin phosphate, stored in phosphate buffer (PB, 0.1 M, chemicals and reagents were obtained from Sigma-Aldrich unless otherwise noted), and maintained at 4° C. Following the second *in vivo* electrophysiological mapping in experimental and sham groups, animals were transcardially perfused and brains were stored as described for acute groups.

Immunohistochemistry

Fixed tissue was sectioned using a vibratome and serial coronal sections 100 μm thick containing the marked border region of S1 were collected and stored in well-plates in 0.1 M PB. Tissue sections containing marks for both the border and medial/lateral marks, or dual-labeled sections, were included in further analyses. Free-floating tissue sections were incubated in 5 % Normal Goat Serum and 0.5% Triton-X 100 at room temperature, then incubated with commercially available primary antibodies for BDNF (1:50 dilution, AbCam, Rabbit polyclonal primary antibody to BDNF, ab6201) or TrkB (1:100 dilution, AbCam, Rabbit polyclonal primary antibody to TrkB, ab51190) overnight at 4° C. Sections were rinsed with PB before application of the fluorescently conjugated secondary antibodies (20 nM concentration, Cy5 donkey anti-rabbit), and kept covered for three hours at room temperature. A total of 5 sections per brain were stained for analysis. In addition to two primary and secondary antibody stained sections (Fig. 2), two control sections were included; one control section received primary, but no secondary antibody (Fig. 3), and the other received secondary antibody but no primary antibody (Fig. 4). One section per brain was stained with SYTOX Green (Molecular Probes) cell stain for laminar analysis (Fig. 5); SYTOX Green (150 μL, 1 μM SYTOX Green in 15 mM HEPES buffer) was applied to sections at room temperature for 10 min, then rinsed with PB. All five sections were then stepped in glycerol (70 % and 90 %, glycerol in PB) and mounted in 90 % glycerol (with 4 % N-propyl-gallate to prevent fading of the fluorescence) on glass slides, coverslipped, sealed, and stored at -20 ° C.

Image Acquisition and Analysis

All images were acquired using the Zeiss confocal laser-scanning microscope (LSM510) in the Central Facility for Advanced Microscopy and Microanalysis (CFAMM). Z-stack images

(optical slice depth 40-90 μm), taken at 10x magnification (0.7 zoom, 512 x 512 frame size, scan speed 4), were acquired for stained and control sections using the appropriate configuration settings for DiI, DiO, Cy5, SYTOX Green (single-track; Rhodamine filter, FITC/Rhodamine, Cy5, FITC/Rhodamine, respectively). Detector gain and amplifier offset were adjusted to set the background, reduce noise, and avoid saturation using the range indicator (Fig. 6). Three z-stack images were acquired for each tissue section, one containing dye marks, and two of the antibody or SYTOX Green staining to capture layers I-VI. In control sections, only two images were acquired, one containing dye marks, and one of the antibody staining (Fig. 3, 4); all settings including gain and offset were maintained between analysis and control sections. Using the LSM510 Browser (Zeiss), each image was projected (first angle 0, projections 1, difference angle 0, maximum transparency), a scale bar added, and exported (.Tif file format). Images were composited using Photoshop CS3 (Adobe Systems, Inc.). Corel Painter X (Corel Corporation) was used to create analysis boxes 100 μm wide positioned on either side of both border and medial/lateral dye marks (Fig. 2). Dimensions of analysis boxes correspond to laminar distribution as assessed by Sytox Green staining (Fig. 5). A total of 20 boxes were created for each tissue section, 10 analysis boxes representing the border and 10 boxes representing a location 500 μm from the border in the forepaw or lower jaw representation (Fig. 2). Mean pixel intensity was then determined for each box using the Wide Histogram plug-in (Reindeer Graphics, Inc.) for Photoshop CS3.

Mean pixel intensity data was collected from processed micrograph images and analyzed using Photoshop CS3, Excel (Microsoft), and SPSS Statistics 17.0 software package (SPSS, Inc.). For each analysis box (Fig. 2), blue channel histogram mean ($\overline{X}$), standard deviation (σ), median (Med) and pixel count was recorded, and data was downloaded. Cell counts were

obtained for boxes using trained judges kept blind to experimental condition, final cell counts were averaged across judges; interobserver agreement (IOA) was calculated (number of agreements/number of agreements + disagreements x 100) and counts were discarded if IOA fell below 70 %. Descriptive and inferential statistical analyses were then conducted including planned independent and paired student's *t*-tests (significance level $\alpha = 0.05$). Independent *t*-tests were conducted to (1.) compare the difference in mean pixel intensity between stained and control tissue sections, (2.) assess overall differences in staining intensity at the border and within the forepaw and lower jaw representations, (3.) compare the mean pixel intensity of boxes on either side of a dye mark at the border, and forepaw or lower jaw representation (e.g., Fig. 2 columns E and F, compared to G and H). Planned comparisons also included an examination of mean pixel intensity by layer, within the forepaw and lower jaw representations compared to the border (e.g., Fig. 2 assessing differences in layers I-VI in columns E and F, compared to G and H). Independent student's *t*-tests were also conducted to examine the general and layer specific differences in BDNF antibody staining in the forepaw compared to lower jaw representation.

Results

BDNF Antibody and SYTOX Green Staining in Acute Controls

Analysis of BDNF antibody staining (Fig. 2) provides support for the expression of BDNF in S1 (n = 8 stained tissue sections from 5 animals, 3 sections containing lower jaw, and 5 forepaw); initial tests were conducted to examine overall differences in mean pixel intensity at the border, and 500 μm within the forepaw and lower jaw representations. Comparisons of antibody labeling at the border and within the forepaw and lower jaw representations in normal acute controls (Fig. 7, data pooled from analysis boxes in layers I-VI), revealed a statistically significant difference in fluorescent antibody labeling of BDNF at the border compared to a site

500 μm within the lower jaw representation (t = -2.870, df = 110; p = 0.005, two-tailed); greater mean pixel intensity, indicating a higher level of antibody staining, was observed within the lower jaw representation. Although the difference in mean staining intensity between the border and 500 μm medial in the forepaw representation (Fig. 7), failed to reach statistical significance (t = -1.894, df = 126; p = 0.060, two-tailed), a trend was observed suggesting increased mean pixel intensity in the forepaw representation.

Results support general laminar differences in BDNF antibody staining in layers I-VI (Fig. 8, data pooled from analysis boxes E-H, Fig. 2), as well as layer specific differences in staining at the border and within forepaw and lower jaw representations (Fig. 9, data pooled from boxes E, F, and G, H; Fig. 2). Independent student's *t*-tests revealed overall statistically significant differences in mean pixel intensity in layers I-IV (Fig. 9), but no differences in layers V and VI (values of *t*-tests given in Table 1); similar differences in laminar distribution were found at the border, and within forepaw and lower jaw representations (Fig. 10, values of *t*-tests given in Table 2).

To investigate the impact of the dye mark on antibody staining distributions (Fig. 11), mean pixel intensity was analyzed in boxes located on either side of a dye deposit marking the location of the lower jaw or forepaw representation (columns E, F, and G, H, were compared, Fig. 2), analysis included layers extending well below the mark itself. Independent student's *t*-tests were conducted comparing columns E and F, and G and H (Fig. 2); results of these analyses revealed no statistically significant difference (Fig. 11) in mean pixel intensity of BDNF antibody staining on either side of the dye mark at the border or within the lower law and forepaw representations (border t = -1.544, df = 78; p = 0.127, two-tailed; forepaw t = 0.496, df = 46; p = 0.0.622, two-tailed; lower jaw t = 0.094, df = 30; p = 0.926, two-tailed).

Discussion

Using a model system which allows us to induce cortical reorganization and study the plasticity of cortical sensory representations, we are able to investigate the mechanisms involved in these changes using, anatomical, physiological, and immunohistochemical techniques. Data collection is currently in progress, and many questions remain concerning potential differences in staining patterns that may be observed between experimental and sham groups, as well as differences between BDNF and TrkB antibody labeling across groups. These preliminary results and initial findings provide support for the continued study of BDNF and TrkB during cortical reorganization.

The initial analyses of BDNF antibody staining in the acute control group indicate several trends in BDNF antibody staining of border, forepaw and lower jaw representations in layers I-VI. Layer specific changes were observed that indicate the greatest levels of staining were located in superficial layers, it was noted that mean pixel intensity was progressively diminished in deeper layers (Fig. 8). Investigations concerning the potential influence of the dye mark on distribution of antibody staining do not indicate that the dye mark alone has any significant influence the distribution of BDNF antibody staining in acute controls (Fig. 11). Dramatic layer specific reductions in mean pixel intensity were observed at the border, and in lower jaw and forepaw representations (Figs. 9, 10). Results of previous research investigating BDNF and TrkB, using immunohistochemical techniques and quantification of labeled somata, have shown high expression of BDNF and TrkB in layers I-III, V, and VI (Yan et al., 1997a, 1997b; Miller and Pitts, 2000; Pitts and Miller, 2000). Although the present study supports high levels of staining in layers II/III, we observed little staining in layers V and VI (Figs. 8-10). These findings may be explained by the current image acquisition protocol which maintains the gain

and offset settings between individual images, but relies on initial settings from images centered on the dye marks in superficial layers. We continue to work towards optimization of the data acquisition and analysis protocol to reduce potential measurement error, by creating standardized image acquisition and processing protocol.

Previous research provides support for the involvement of BDNF and high-affinity receptor TrkB in many roles during development and growth as well as in the maintenance and survival of cells within the CNS (Prakash et al., 1996; Yan et al., 1997b; Huang and Reichardt, 2001; Lipsky and Marini, 2007). Studies of cortical reorganization highlight many changes in the structure and function of neurons with the reorganized and surrounding cortical regions (Hickmott and Merzenich, 1998, 2002; Hickmott, 2005). Previous studies have reported anatomical and physiological changes such as the growth of axons, remodeling of dendrites, and changing bias of representational borders during reorganization of S1 (Hickmott and Merzenich, 1998, 1999, 2002; Hickmott and Steen, 2005). BNDF and TrkB signaling may be involved in the processes that bring about these wide spread changes. The current study was designed to investigate the role of BDNF and TrkB during reorganization of S1, although preliminary results are promising, further data collection and analysis is necessary before drawing conclusions.

Future analyses of experimental and sham groups will reveal potential differences in BDNF and TrkB antibody staining, as well as how these staining patterns change over time through the examination of 3-day, 7-day, and 14-day time points. Investigations at these time points will allow is to examine immediate changes taking place during reorganization, as well as look at changes as reorganized regions become stable. In future experiments, it would be interesting examine the changes taking place immediately following mapping and peripheral denervation by looking at time points 1-3 hours following a denervation or sham-denervation

procedure. In future experiments, we will explore combinations of BDNF and TrkB antibody staining and SYTOX Green staining within the same tissue section; this would allow us to estimate cell density and quantify the percentage of cells expressing BDNF and TrkB within the same tissue section. It would also be interesting to attempt to prevent reorganization by exogenous application or infusion of BDNF or TrkB scavengers. Future studies incorporating transgenic BDNF or TrkB mutatant mice may also provide more support for the role of BDNF and TrkB during reorganization of cortical sensory maps.

Neural plasticity and cortical reorganization have been well studied in the sensory systems (Calia et al., 1998; Cheetham et al., 2007, 2008; Irvine, 2007; Oh et al., 2007; Tan et al., 2007); this research highlights the ability of the mammalian brain to adapt to changes in peripheral sensory input following altered sensory experience, injury, or trauma (Steffen and Van der Loos, 1980; Jain et al., 1998; Oh et al., 2007, Tan et al., 2007). The mechanisms that underlie this plasticity apply more broadly to the neural plasticity involved in learning and memory, and an enhanced knowledge of these mechanisms will ultimately lead to applications in rehabilitation from stroke and trauma (Bracewell, 2003; Acerra et al., 2007; Gauthier et al., 2008), to new treatments for disorders such as phantom limb pain (MacIver et al., 2008), as well as interventions designed to enhance learning and memory.

Acknowledgements

This research was supported by a COR grant and Academic Senate funds, from the University of California, Riverside. I would like to acknowledge my esteemed advisor and Committee Chair, Dr. Peter Hickmott, and thank him for his guidance, encouragement, patience, and wisdom. I would also like to thank my distinguished committee members Dr. Michael Adams and Dr. Khaleel Razak for their time and support. Furthermore, I would like to acknowledge my erudite lab mates Andrea Nolen and Jeff Paullus for welcoming me to the lab and generously sharing the secrets to their success. I would like to thank Dr. David Carter for sharing his expertise in the field of confocal microscopy. Thank you all for your time and support.

Figure 1.

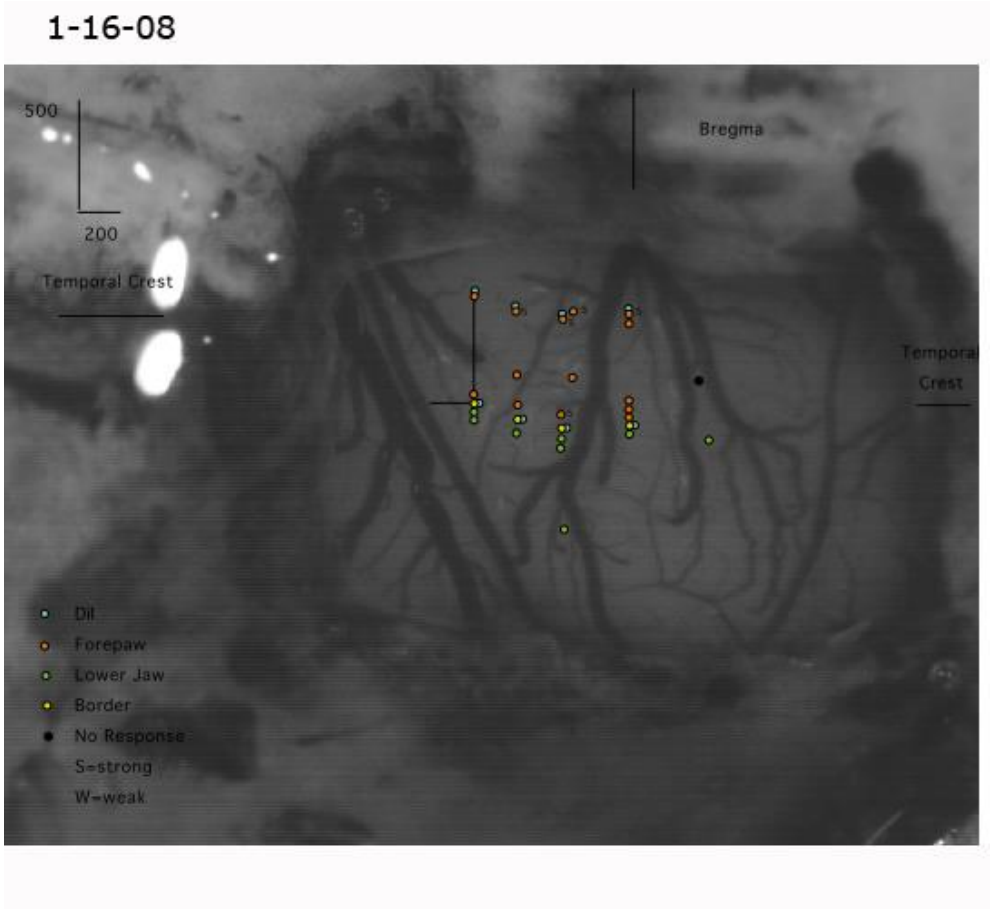

Figure 1. Photomicrograph (2x magnification) of the cortical surface was taken with Pixera software, and colored shapes were overlaid using Canvas 5 software to indicate the sites of electrode penetrations during *in vivo* electrophysiological mapping. Dorsal to the top, caudal to the left, rostral to the right. Scale bars indicate lines 500 μm and 200 μm. Responses were elicited by tactile stimulation of the forepaw and lower jaw with a slender glass probe; and colored markers placed on the micrograph corresponding to response category. Responses were categorized and indicated on maps as follows: lower jaw (green), border (yellow), forepaw (orange), no response (black); DiI marks are indicated by blue.

Figure 2.

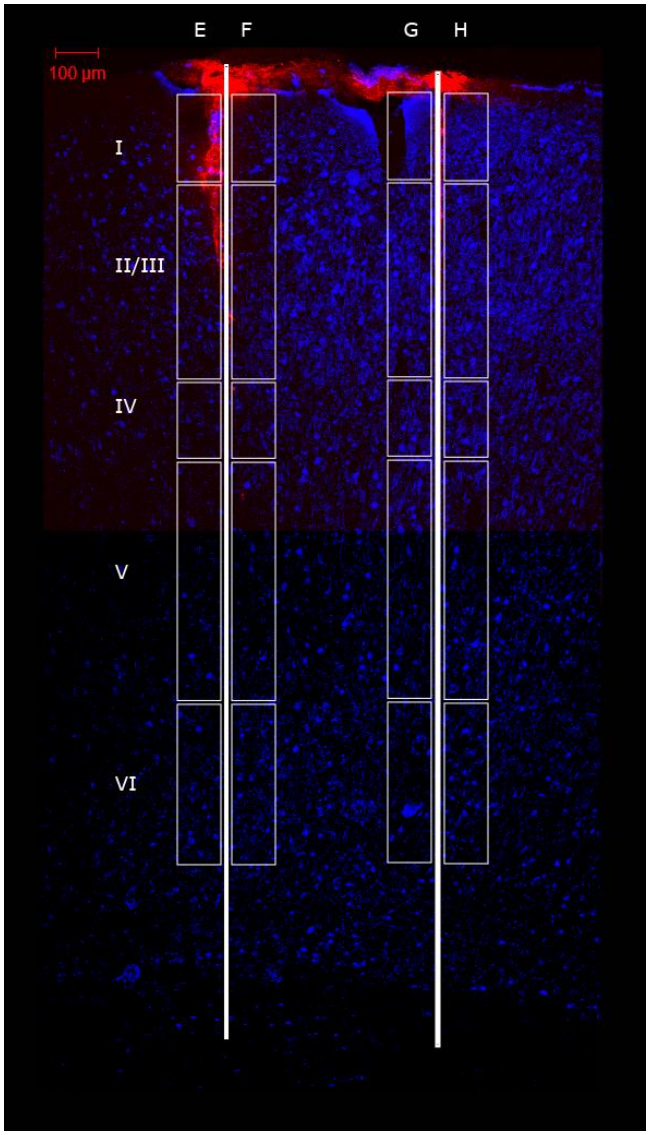

Figure 2. Analysis box layout in tissue sections stained for BDNF. Image shown is a coronal tissue section of S1, DiI marks indicate the border (right) between the lower jaw and forepaw, and a site 500 μm within the forepaw (left) representation. Tissue was stained with BDNF primary antibody (1:50 dilution), Cy5 secondary antibody (20 nM concentration). Image indicates that BDNF is present in S1 distributed throughout cortical layers. Pial surface is at the top of image, medial to the left and lateral to the right. Analysis boxes 100 µm wide are placed on either side of a dye mark using Corel Painter X, dimensions correspond to average laminar distribution as assessed by SYTOX Green staining (Fig. 5). Scale bar = 100 μm.

Figure 3.

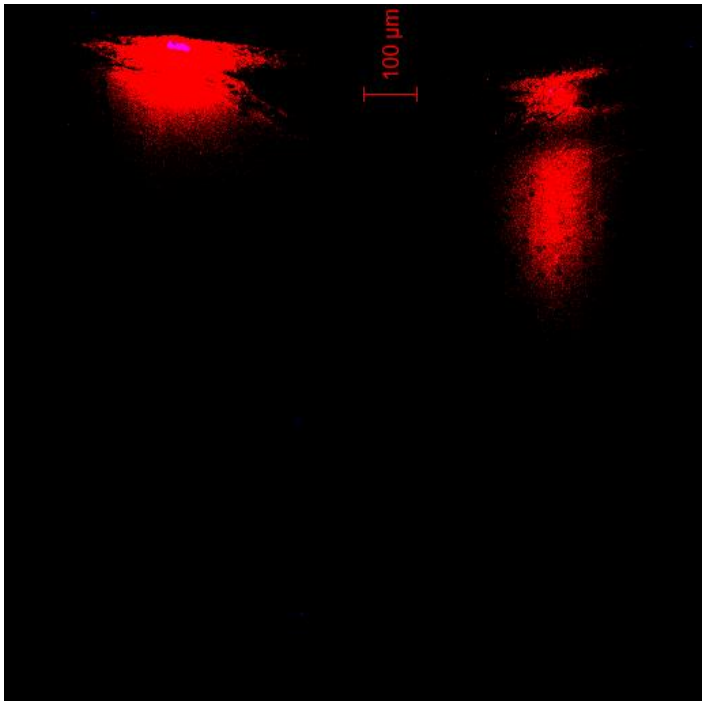

Figure 3. Photomicrograph of control tissue section from S1; stained with primary BDNF antibody, but no secondary Cy5 antibody. DiI marks indicate the border (right) and 500 μm within the forepaw (left) representation (10x magnification, 0.7 zoom). Pial surface is at the top of image, medial to the left and lateral to the right; scale bar represents100 μm. Detector gain, amplifier offset, and all other parameters maintained between analysis and control images. Image indicates little to no fluorescent signal in control sections compared to stained analysis (used to assess potential autofluorescence).

Figure 4.

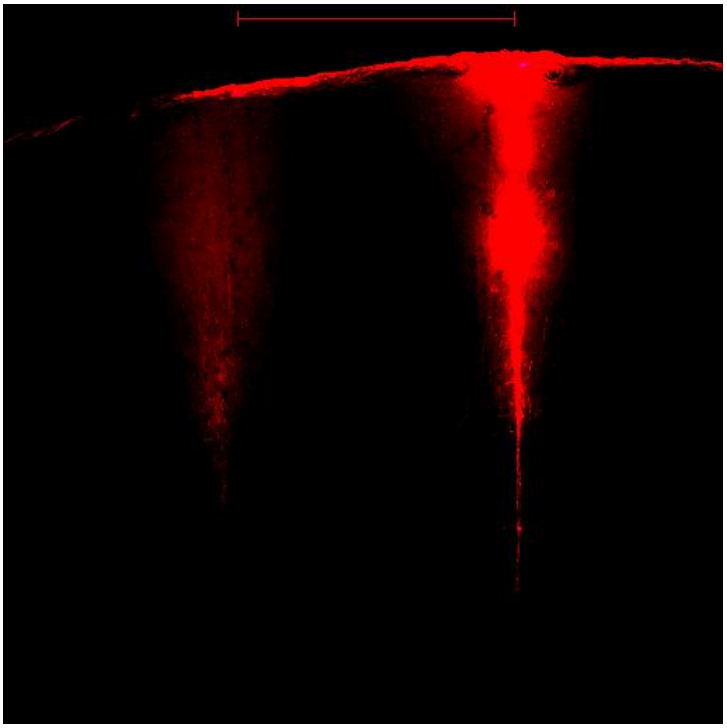

Figure 4. Photomicrograph of control tissue section; stained with secondary Cy5 antibody, but no primary BDNF antibody. Coronal tissue section taken from S1, DiI marks indicate the border (right), and 500 μm within the forepaw (left) representation (10x magnification, 0.7 zoom). Pial surface is at the top of image, medial to the left and lateral to the right; scale bar represents 500 μm. Detector gain, amplifier offset, and all other parameters maintained between analysis and control images. Image indicates little to no fluorescent signal in control sections compared to stained analysis (used to assess nonspecific binding of secondary Cy5 antibody).

Figure 5.

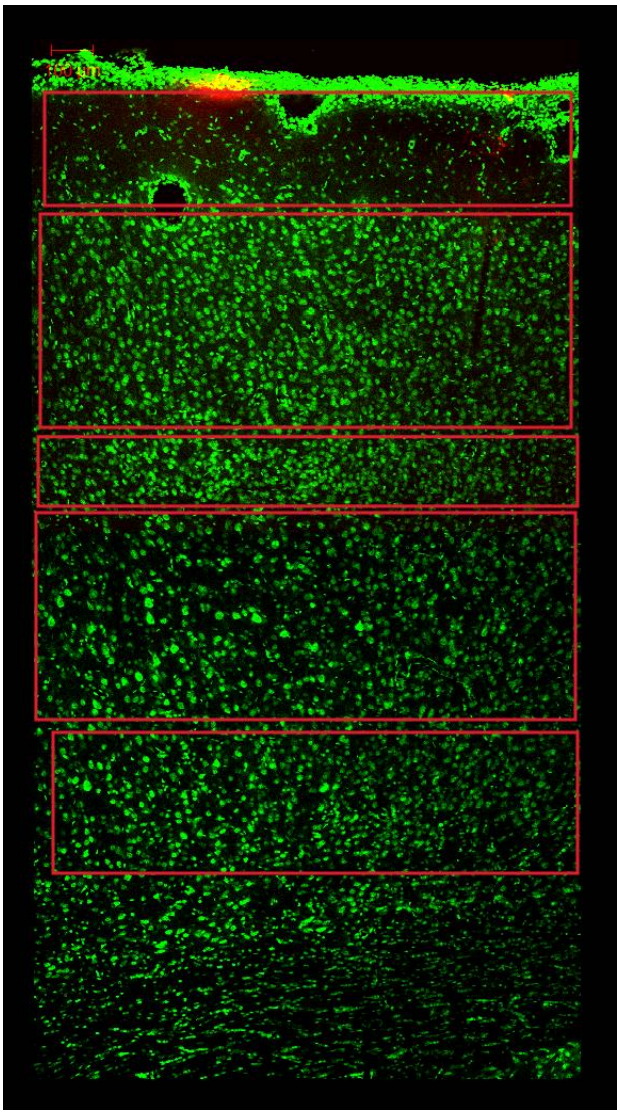

Figure 5. SYTOX Green nuclear stain analysis was conducted to determine average dimensions of layers I-VI. Composite photomicrograph image of coronal tissue section stained for SYTOX Green (1 µM). Pial surface is at the top of image, medial to the left and lateral to the right. Boxes representing layers I-VI were created using Corel Painter X based on visual inspection of cell density. Boxes were measured using Corel Painter X and Photoshop CS3, and measurements were averaged across SYTOX Green stained tissue sections (n = 3). Averaged laminar distribution was used to create layer specific analysis boxes for data acquisition (Fig. 2). Scale bar, 100 μm.

Figure 6.

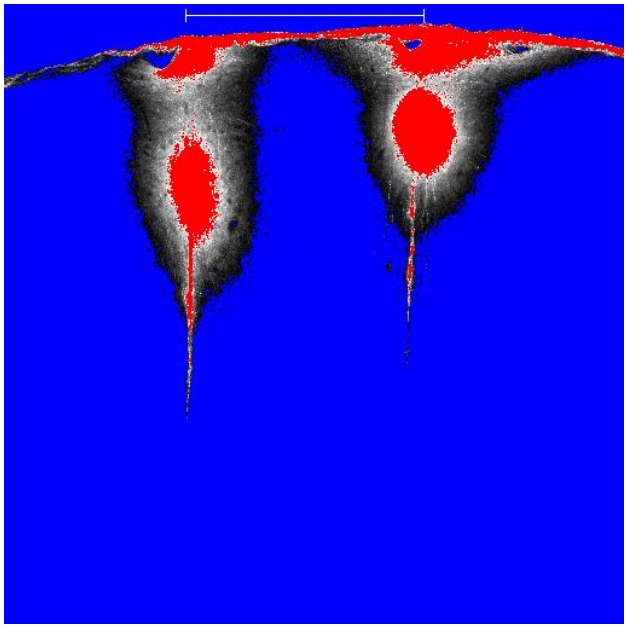

Figure 6. Detector gain and amplifier offset adjustments. Photomicrograph image of tissue section containing two DiI marks. Pial surface is to the top, medial to the left, lateral to the right. Scale bar represents 500 μm. Using the range indicator, detector gain and amplifier offset are optimized for the dye mark image and readjusted to optimize the initial antibody image in each tissue section. In this image, detector gain (red) was set to capture the lowest portions of the DiI mark, which represent the tip of the recording electrode and the site at which responses were recorded. Amplifier offset (blue) was adjusted until reaching a solid blue background for areas outside of the tissue, top of image.

Figure 7.

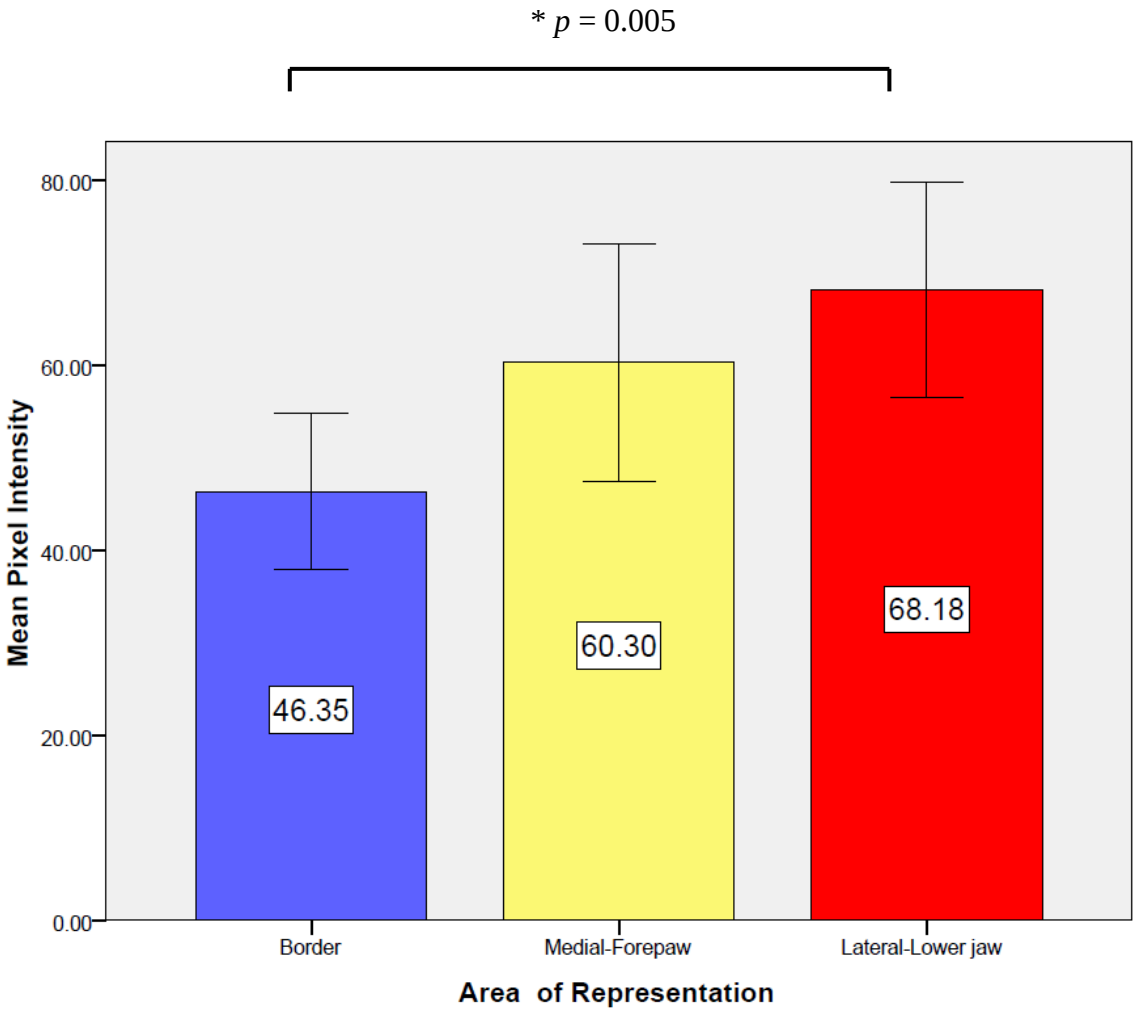

Figure 7. Mean pixel intensity of BDNF antibody staining at the border (n = 8 tissue sections taken from 5 animals), and within the forepaw (n = 5 tissue sections) and lower jaw representations (n = 3 tissue sections). Mean pixel intensity was compared for analysis boxes surrounding DiI marks indicating the border (blue), forepaw (yellow), and lower jaw (red) representations. Colored bars indicate mean pixel intensity of each location collapsed across layers. Asterisk and bar indicate a statistically significance difference between mean pixel intensity at the border compared to the lower jaw representation (α = 0.05 level, p = 0.005). In general, these results reveal a statistically significant difference between BDNF antibody staining at the border compared to the lower jaw representation. Numbers within bars indicate the mean pixel intensity for all analysis boxes located at the border, and in forepaw and lower jaw representations.

Figure 8.

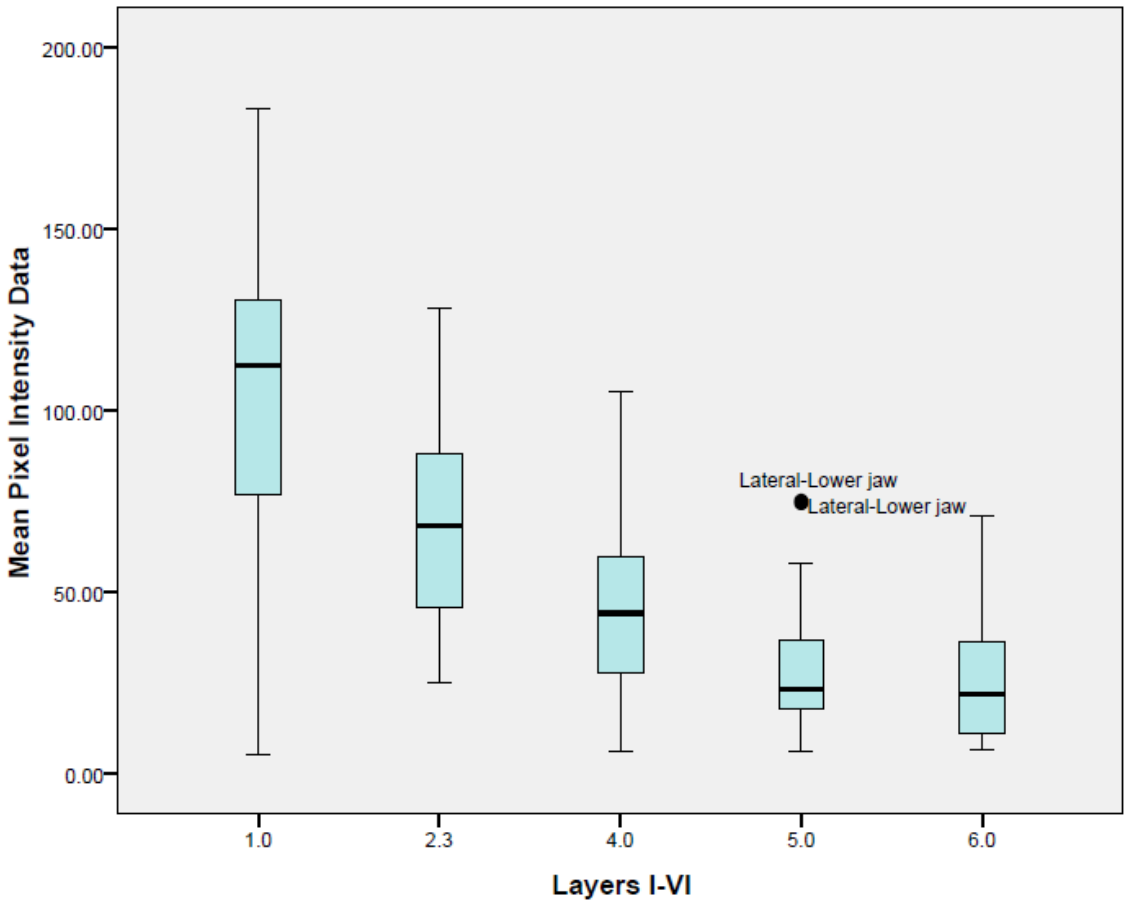

Figure 8. Layer specific changes in BDNF antibody staining distribution. Box plot graph depicting mean pixel intensity across all analysis sections (n = 8 tissue sections taken from 5 animals containing 3 lower jaw, 5 forepaw, and 8 border sites) in layers I-VI (data pooled from boxes E-H; Fig. 2). Mean intensity decreases from superficial to deep layers. Each box represents a given layer, upper and lower boundaries of the box illustrate the interquartile range, the line within the box identifies mean, and bars indicate range of the data set. Note two outliers are found in layer V within the lower jaw representation.

Figure 9.

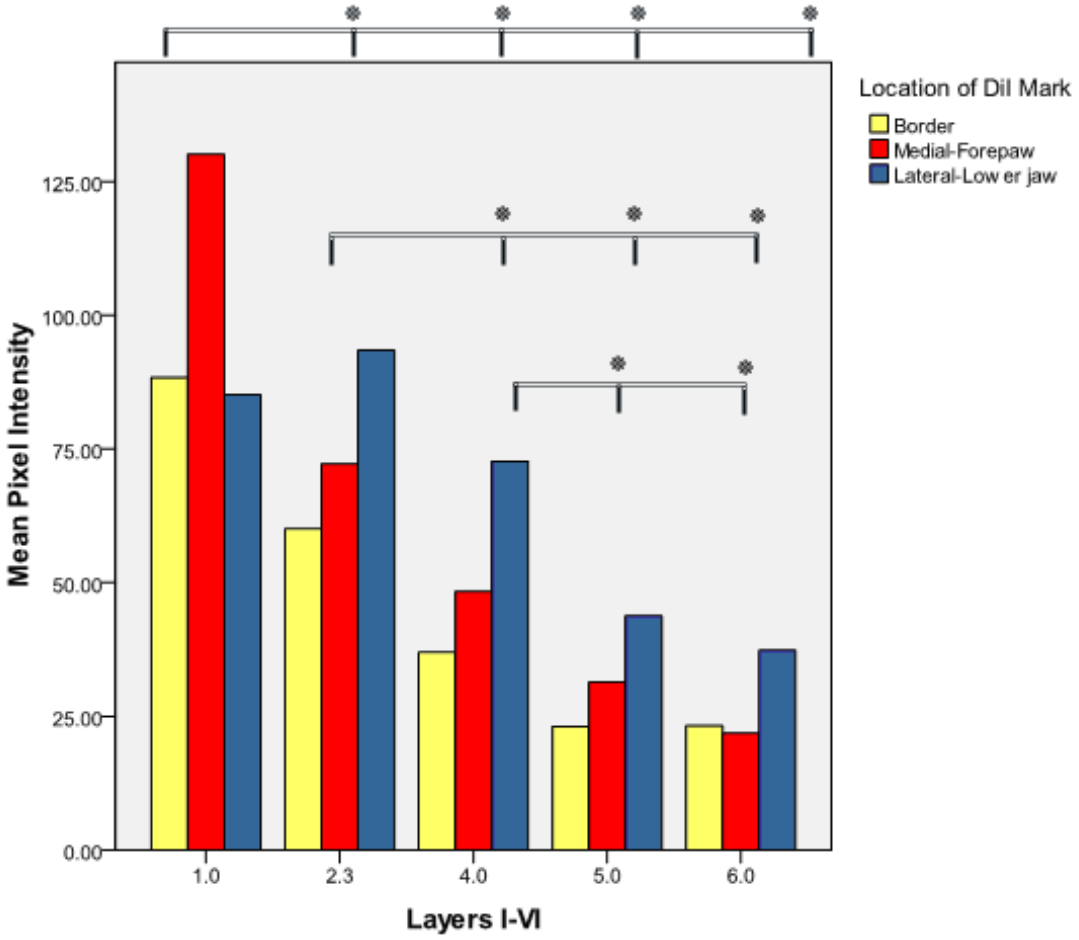

Figure 9. Mean pixel intensity of BDNF antibody staining in layers I-VI at the border, and in forepaw and lower jaw representations. Bars indicate mean pixel intensity (data was pooled from boxes E, F, and G, H; Fig. 2) at the border (yellow), and 500 μm within the forepaw (red) or lower jaw (blue) representations. Independent student's *t*-tests (Table 1.) revealed statistically significant differences ($\alpha = 0.05$) in mean pixel intensity between layers I-IV (data pooled across analysis boxes E-H; Fig. 2), indicated by asterisks ($n = 8$ analysis tissue sections taken from 5 animals containing 3 lower jaw, 5 forepaw, and 8 border sites). Mean pixel intensity decreases from superficial to deeper layers, no statistically significant differences were found between layers V and VI.

Figure 10.

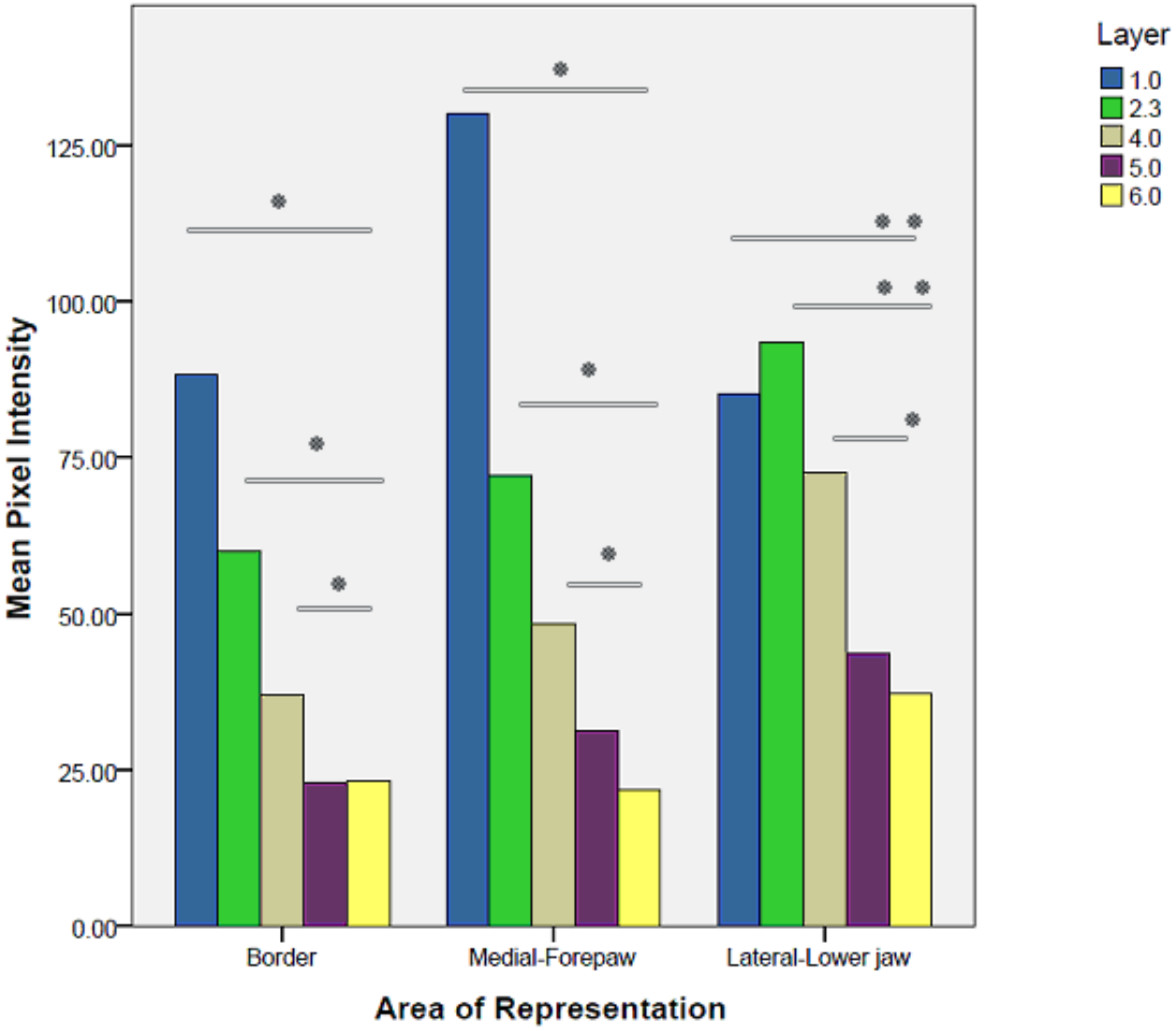

Figure 10. Mean pixel intensity of analysis boxes at the border, and 500 μm within the forepaw and lower jaw representations. Colored bars represent mean pixel intensity of BDNF antibody staining in layers I-VI (data pooled from boxes E, F, and G, H), grouped by area of representation (border, medial-forepaw, or lateral-lower jaw). Statistically significant differences as assessed by independent student's *t*-tests (Table 2.) are marked with asterisks ($\alpha = 0.05$). At the border and in the forepaw and lower jaw representations, statistically significant differences in mean pixel intensity were found between layers I-IV. No statistically significant difference was found between layers V and VI ($n = 8$ stained analysis sections taken from 5 animals containing 3 lower jaw, 5 forepaw, and 8 border sites). Layer I (blue), layer II/III (green), layer IV (light brown), layer V (purple), and layer VI (yellow).

Figure 11

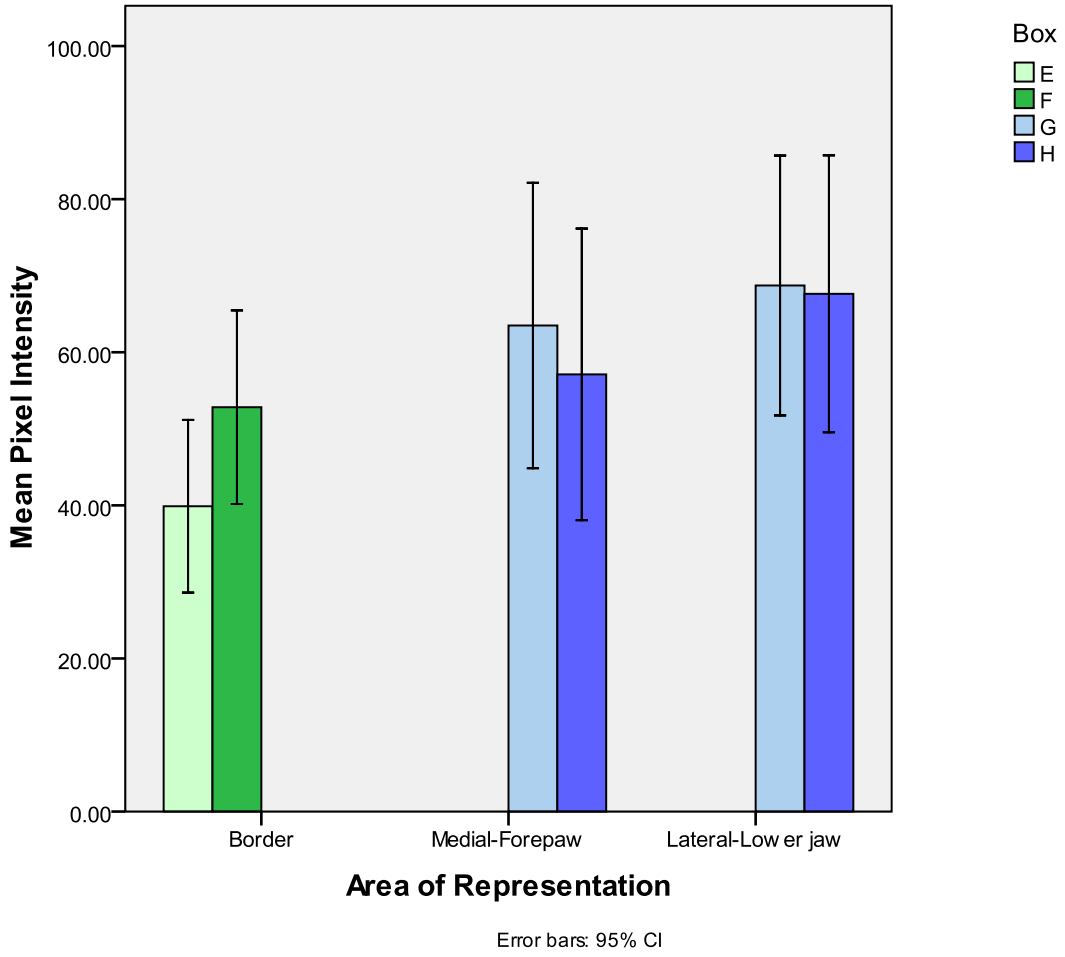

Figure 11. Assessing the influence of the dye mark; examining differences in the distribution of antibody staining at the border and within the forepaw and lower jaw representations. In order to assess the influence of the dye mark, we looked for differences in mean pixel intensity on either side of a dye mark in forepaw and lower jaw representations (500 μm from the border). Each bar represents mean pixel intensity in a given column (data was pooled from analysis boxes in layers I-VI, Fig. 2); E (light green), F (dark green), G (light blue), H (dark blue). Independent student's *t*-tests revealed no statistically significant differences in means located on either side of a dye mark at the border, and in the forepaw and lower jaw representations (n = 8 stained analysis sections taken from 5 animals containing 3 lower jaw, 5 forepaw, and 8 border sites). Error bars indicate the 95 % confidence interval.

Table 1.

BDNF Antibody Staining: Independent Student's *t*-tests Comparisons of Layers I-VI

Comparison	*t* value	*df*	*p* (two-tailed)	Significance (α = 0.05)
Layers I and II/III	3.133	62	0.003	*
Layers I and IV	5.982	62	0.004	*
Layers I and V	8.439	62	0.000	*
Layers I and VI	8.925	62	0.000	*
Layers II/III and IV	3.646	62	0.001	*
Layers II/III and V	7.062	62	0.000	*
Layers II/III and VI	7.751	62	0.000	*
Layers IV and V	3.351	62	0.001	*
Layers IV and VI	4.132	62	0.000	*
Layers V and VI	0.957	62	0.342	

Table 1. BDNF Antibody Staining: Independent Student's *t*-tests Comparisons of Layers I-VI. Table of *t*-test values, degrees of freedom (*df*), exact *p* value provided when possible, significance at the $\alpha = 0.05$ level is indicated by an asterisk (data shown in Fig. 9). Stained analysis sections (n = 8) taken from 5 animals containing 3 lower jaw, 5 forepaw, and 8 border sites.

Table 2.

BDNF Antibody Staining: Independent Student's *t*-tests Comparisons of Layers I-VI at the Border and in the Forepaw and Lower Jaw Representations

Comparison	Location	*t* value	*df*	*p* (two-tailed)	Significance ($\alpha = 0.05$)
Layers I and II/III	Border	1.971	30	0.058	
	Forepaw	4.412	16	0.000	*
	Lower Jaw	-0.639	12	0.535	
Layers I and IV	Border	3.683	30	0.001	*
	Forepaw	8.377	18	0.000	*
	Lower Jaw	0.868	10	0.406	
Layers I and V	Border	4.948	30	0.000	*
	Forepaw	10.502	18	0.000	*
	Lower Jaw	2.806	10	0.019	*
Layers I and VI	Border	4.952	30	0.000	*
	Forepaw	10.824	18	0.000	*
	Lower Jaw	3.212	10	0.009	*
Layers II/III and IV	Border	2.636	30	0.013	*
	Forepaw	2.336	16	0.033	*
	Lower Jaw	1.663	12	0.122	
Layers II/III and V	Border	4.936	30	0.000	*
	Forepaw	4.170	16	0.001	*
	Lower Jaw	3.879	12	0.002	*
Layers II/III and VI	Border	4.963	30	0.000	*
	Forepaw	4.793	16	0.000	*
	Lower Jaw	4.342	12	0.001	*
Layers IV and V	Border	2.065	30	0.048	*
	Forepaw	2.862	18	0.010	*
	Lower Jaw	2.043	12	0.068	
Layers IV and VI	Border	2.067	30	0.047	*
	Forepaw	3.883	16	0.001	*
	Lower Jaw	2.471	10	0.033	*
Layers V and VI	Border	-0.031	30	0.976	
	Forepaw	1.531	18	0.143	
	Lower Jaw	0.436	10	0.672	

Table 1. BDNF Antibody Staining: Independent Student's *t*-tests Comparisons of Layers I-VI at the Border and in the Forepaw and Lower Jaw Representations. Table of *t*-test values, degrees of freedom (*df*), exact *p* value provided when possible, significance at the $\alpha = 0.05$ level is indicated by an asterisk (data shown in Fig. 10). Stained analysis sections (n = 8) taken from 5 animals containing 3 lower jaw, 5 forepaw, and 8 border sites.

References

Acerra NE, Souvlis T, Moseley GL (2007) Stroke, complex regional pain syndrome and phantom limb pain: can commonalities direct future management? J Rehabil Med 39:109-114.

Berardi N, Pizzorusso T, Maffei L (2000) Critical periods during sensory development. Curr Opin Neurobiol 10:138-145.

Bibel M, Barde YA (2000) Neurotrophins: key regulators of cell fate and cell shape in the vertebrate nervous system. Genes Dev 14:2919-2937.

Bracewell RM (2003) Stroke: neuroplasticity and recent approaches to rehabilitation. J Neurol Neurosurg Psychiatry 74:1465.

Cabelli RJ, Allendoerfer KL, Radeke MJ, Welcher AA, Feinstein SC, Shatz CJ (1996) Changing patterns of expression and subcellular localization of TrkB in the developing visual system. J Neurosci 16:7965-7980.

Calford MB (2002) Dynamic representational plasticity in sensory cortex. Neurosci 11:709-738.

Calia E, Persico AM, Baldi A, Keller F (1998) BDNF and NT-3 applied in the whisker pad reverse cortical changes after peripheral deafferentation in neonatal rats. Euro J Neurosci 10:3149-3200.

Cheetham CE, Hammond MS, Edwards CE, Finnerty GT (2007) Sensory experience alters cortical connectivity and synaptic function site specifically. J Neurosci 27:3456-3465.

Daw MI, Scott HL, Isaac JT (2007) Developmental synaptic plasticity at the thalamocortical input to barrel cortex: mechanisms and roles. Mol Cell Neurosci 34:493-502.

Dechant G, Barde YA (1997) Signalling through the neurotrophin receptor p75NTR. Curr Opin Neurobiol 7:413-418.

DiCarlo JJ, Lane JW, Hsiao SS, Johnson KO (1996) Marking microelectrode penetrations with fluorescent dyes. J Neurosci Methods 64:75-81.

Flor H, Nikolajsen L, Staehelin JT (2006) Phantom limb pain: a case of maladaptive CNS plasticity? Nat Rev Neurosci. 7:873-81.

Gauthier LV, Taub E, Perkins C, Ortmann M, Mark VW, Uswatte G (2008) Remodeling the brain: plastic structural brain changes produced by different motor therapies after stroke. Stroke 39:1520-1525.

Gillespie DC, Crair MC, Stryker MP (2000) Neurotrophin-4/5 alters responses and blocks the effect of monocular deprivation in cat visual cortex during the critical period. J Neurosci 20:9174-9186.

Hempstead BL (2002) The many faces of p75NTR. Curr Opin Neurobiol 12:260-267.

Hickmott PW (2005) Changes in intrinsic properties of pyramidal neurons in adult rat S1 during cortical reorganization. J Neurophysiol 94:501-11.

Hickmott PW, Ethell IM. (2006) Dendritic plasticity in the adult neocortex. Neuroscientist 12:16-28.

Hickmott PW, Merzenich MM (1998) Single-cell correlates of a representational boundary in rat somatosensory cortex. J Neurosci 18:4403-4416.

Hickmott PW, Merzenich MM (1999) Dendritic bias of neurons in rat somatosensory cortex associated with a functional boundary. J Comp Neurol 409:385-399.

Hickmott PW, Merzenich MM (2002) Local circuit properties underlying cortical reorganization. J Neurophysiol 88:1288-1301.

Hickmott PW, Steen PA (2005) Large-scale changes in dendritic structure during reorganization of adult somatosensory cortex. Nat Neurosci 8:140-142.

Huang EJ, Reichardt LF (2001) Neurotrophins: roles in neuronal development and function. Annu Rev Neurosci 24:677-736.

Inagaki T, Begum T, Reza F, Horibe S, Inaba M, Yoshimura Y, Komatsu Y (2008) Brain-derived neurotrophic factor-mediated retrograde signaling required for the induction of long-term potentiation at inhibitory synapses of visual cortical pyramidal neurons. Neurosci Res 61:192-200.

Irvine DR (2007) Auditory cortical plasticity: does it provide evidence for cognitive processing in the auditory cortex? Hear Res 229:158-170.

Jain N, Florence SL, Kaas JH (1998) Reorganization of somatosensory cortex after nerve and spinal cord injury. News Physiol Sci 13:143-149.

Kaas JH (2008) The evolution of the complex sensory and motor systems of the human brain. Brain Res Bull 75:384-390.

Kaneko M, Hanover JL, England PM, Stryker MP (2008) TrkB kinase is required for recovery, but not loss, of cortical responses following monocular deprivation. Nat Neurosci 11:497-504.

Lindsay RM, Weigand SJ, Altar CA, DiStefano PS (1994) Neurotrophic factors: from molecule to man. Trends Neurosci 17:182-190.

Lipsky RH, Marini AM (2007) Brain-derived neurotrophic factor in neuronal survival and behavior-related plasticity. Ann N Y Acad Sci 1122:130-143.

Lotze M, Flor H, Grodd W, Larbig W, Birbaumer N (2001) Phantom movements and pain. An fMRI study in upper limb amputees. Brain 124:2268-2277.

Lu B (2003) BDNF and activity-dependent synaptic modulation. Learn Mem 10:86–98.

Ludlow CL, Hoit J, Kent R, Ramig LO, Shrivastav R, Strand E, Yorkston K, Sapienza CM (2008) Translating principles of neural plasticity into research on speech motor control recovery and rehabilitation. J Speech Lang Hear Res 51:S240-S258.

Lush ME, Ma L, Parada LF (2005) TrkB signaling regulates the developmental maturation of the somatosensory cortex. Int J Devl Neurosci 23:523–536.

MacIver K, Lloyd DM, Kelly S, Roberts N, Nurmikko T (2008) Phantom limb pain, cortical reorganization and the therapeutic effect of mental imagery. Brain 131:2181-91.

Markham JA, Greenough WT (2004) Experience-driven brain plasticity: beyond the synapse. Neuron Glia Biol 1:351-363.

McAllister AK (2000) Cellular and molecular mechanisms of dendrite growth. Cereb Cortex 10:963-973.

McAllister AK (2001) Neurotrophins and neuronal differentiation in the central nervous system. Cell Mol Life Sci 58:1054-1060.

Miller MW, Pitts FA (2000) Neurotrophin receptors in the somatosensory cortex of the mature rat: co-localization of p75, trk, isoforms and c-neu. Brain Res 852:355-366.

Moore CI, Stern CE, Dunbar C, Kostyk SK, Gehi A, Corkin S (2000) Referred phantom sensations and cortical reorganization after spinal cord injury in humans. Proc Natl Acad Sci USA. 97:14703-14708.

Nagappan G, Lu B (2005) Activity-dependent modulation of the BDNF receptor TrkB: mechanisms and implications. Trends Neurosci 28:464-471.

Oh SH, Kim CS, Song JJ (2007) Gene expression and plasticity in the rat auditory cortex after bilateral cochlear ablation. Acta Otolaryngol 127:341-350.

Petersen CC, Sakmann B (2000) The excitatory neuronal network of rat layer 4 barrel cortex. J Neurosci 20:7579-7586.

Pitts AF, Miller MW (2000) Expression of nerve growth factor, brain-derived neurotrophic factor, and neurotrophin-3 in the somatosensory cortex of the mature rat: coexpression with high-affinity neurotrophin receptors. J Comp Neurol 418:241-254.

Prakash N, Cohen-Cory S, Frostig RD (1996) Rapid and opposite effects of BDNF and NGF on the functional organization of the adult cortex in vivo. Nature 381:702-706.

Rosa MG, Tweedale R (2005) Brain maps, great and small: lessons from comparative studies of primate visual cortical organization. Philos Trans R Soc Lond B Biol Sci 360:665-91.

Schreiner CE, Winer JA (2007) Auditory cortex mapmaking: principles, projections, and plasticity. Neuron 6:356-365.

Shieh PB, Ghosh A (1999) Molecular mechanisms underlying activity-dependent regulation of BDNF expression. J Neurobiol 41:127-134.

Silver MA, Fagiolini M, Gillespie DC, Howe CL, Frank MG, Issa NP, Antonini A, Stryker MP (2001) Infusion of nerve growth factor (NGF) into kitten visual cortex increases immunoreactivity for NGF, NGF receptors, and choline acetyltransferase in basal forebrain without affecting ocular dominance plasticity or column development. Neurosci 108:569-585.

Singh TD, Mizuno K, Kohno T, Nakamura S (1997) BDNF and trkB mRNA expression in neurons of the neonatal mouse barrel field cortex: normal development and plasticity after cauterizing facial vibrissae. Neurochem Res 22:791-797.

Sofroniew MV, Howe CL, Mobley WC (2001) Nerve growth factor signaling, neuroprotection, and neural repair. Annu Rev Neurosci 24:1217-1281.

Steen PA, Mason M, Pham L, Lefebvre Y, Hickmott PW (2007) Axonal bias at a representational border in adult rat somatosensory cortex (S1). J Comp Neurol 500:634-45.

Steffen H, Van der Loos H (1980) Early lesions of mouse vibrissal follicles: their influence on dendrite orientation in the cortical barrelfield. Exp Brain Res 40:419-31.

Tan J, Rüttiger L, Panford-Walsh R, Singer W, Schulze H, Kilian SB, Hadjab S, Zimmermann U, Köpschall I, Rohbock K, Knipper M (2007) Tinnitus behavior and hearing function correlate with the reciprocal expression patterns of BDNF and Arg3.1/arc in auditory neurons following acoustic trauma. Neurosci 145:715-726.

Van der Loos H, Woolsey TA (1973) Somatosensory cortex: structural alterations following early injury to sense organs. Science 179:395-398.

Woodhouse A (2005) Phantom limb sensation. Clin Exp Pharmacol Physiol 32:132-134.

Woolsey TA, Welker C, Schwartz RH (1975) Comparative anatomical studies of the SmL face cortex with special reference to the occurrence of "barrels" in layer IV. J Comp Neurol 164:79-94.

Yan Q, Radeke MJ, Matheson CR, Talvenheimo J, Welcher AA, Feinstein SC (1997a) Immunocytochemical localization of TrkB in the central nervous system of the adult rat. J Comp Neurol 378:135-157.

Yan Q, Rosenfeld RD, Matheson CR, Hawkins N, Lopez OT, Bennett L, Welcher AA (1997b) Expression of brain-derived neurotrophic factor protein in the adult rat central nervous system. Neurosci 78:431-448.

Zhang YH, Chi XX, Nicol GD (2008) Brain-derived neurotrophic factor enhances the excitability of rat sensory neurons through activation of the p75 neurotrophin receptor and the sphingomyelin pathway. J Physiol 586:3113-3127.